

pubs.acs.org/JACS Article

Janus Cross-links in Supramolecular Networks

Swagata Mondal, Jacob J. Lessard, Chhuttan L. Meena, Gangadhar J. Sanjayan,* and Brent S. Sumerlin*



Cite This: J. Am. Chem. Soc. 2022, 144, 845-853



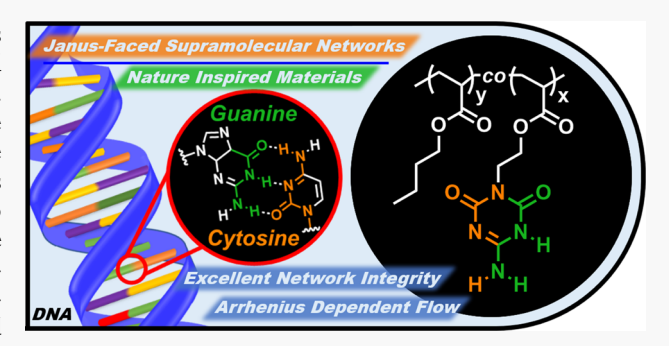
ACCESS

Metrics & More

Article Recommendations

Supporting Information

ABSTRACT: Thermosets composed of cross-linked polymers demonstrate enhanced thermal, solvent, chemical, and dimensional stability as compared to their non-cross-linked counterparts. However, these often-desirable material properties typically come at the expense of reprocessability, recyclability, and healability. One solution to this challenge comes from the construction of polymers that are reversibly cross-linked. We relied on lessons from Nature to present supramolecular polymer networks comprised of cooperative Janus-faced hydrogen bonded cross-links. A triazine-based guaninecytosine base (GCB) with two complementary faces capable of selfassembly through three hydrogen bonding sites was incorporated into poly(butyl acrylate) to create a reprocessable and recyclable



network. Rheological experiments and dynamic mechanical analysis (DMA) were employed to investigate the flow behavior of copolymers with randomly distributed GCB units of varying incorporation. Our studies revealed that the cooperativity of multiple hydrogen bonding faces yields excellent network integrity evidenced by a rubbery plateau that spanned the widest temperature range yet reported for any supramolecular network. To verify that each Janus-faced motif engages in multiple cross-links, we studied the effects of local concentration of the incorporated GCB units within the polymer chain. Mechanical strength improved by colocalizing the GCB within a block copolymer morphology. This enhanced performance revealed that the number of effective cross-links in the network increased with the local concentration of hydrogen bonding units. Overall, this study demonstrates that cooperative noncovalent interactions introduced through Janus-faced hydrogen bonding moieties confers excellent network stability and predictable viscoelastic flow behavior in supramolecular networks.

INTRODUCTION

The synthesis of robust polymer materials is typically achievable through covalent cross-linking of polymer chains to generate a network that spans the entire sample; however, the fixity that is the hallmark of these "thermosets" comes at a cost. The network structure of these materials prevents the separation and reptation of chains, by both solvation and heating, making these materials unrecyclable by conventional methods (e.g., direct mechanical reprocessing). As the development of plastics with recyclability has become a necessity in modern polymer manufacturing, this prerequisite for materials becomes increasingly difficult when durability in harsh environments (e.g., high temperatures) is also required. Significant efforts have been made to exploit reversible crosslinks in either supramolecular or covalent adaptable networks (CANs), wherein the links between chains can be broken and reformed.²⁻¹² These dynamic networks have been described in terms of the mechanism of exchange and the nature of their cross-links; supramolecular networks rely on noncovalent interactions while CANs are comprised of reversible covalent bonds. 13-17

The mechanism of exchange for CANs can be described as associative or dissociative. 2 Dissociative CANs demonstrate network reversibility through sequential and discrete bond dissociation and association steps. In associative CANs (e.g., "vitrimers"), these steps occur simultaneously when a reactive moiety within the network undergoes a substitution or metathesis reaction with an existing cross-link, such that a new cross-link is formed simultaneous to the initial cross-link dissociating. These mechanistic differences produce profound diversity in the processablilty and application of these materials. At high temperatures, dissociative CANs favor bond dissociation and can be tailored to transition to an uncross-linked viscoelastic fluid at a desired temperature. 18 On the other hand, simultaneous bond exchange in associative CANs limits de-cross-linking to maintain a constant cross-link density at all temperatures. However, as has been recently highlighted, dissociative networks can also be designed to preserve high cross-link density over vast temperature

Received: October 7, 2021 Published: January 5, 2022





ranges. 13,19 Indeed, the balance of fixity and cross-link reversibility for strategically designed dissociative CANs allows for a wide array of conditions and techniques for reprocessing. 19,20

Supramolecular networks can also combine increased strength and reprocessability via transient highly directional interactions like hydrogen bonding, metal-ligand coordination, $\pi - \pi$ interaction, and host-guest complexation among others. 21,22 Network formation is achieved through the noncovalent cross-linking of polymer backbones or through supramolecular polymerization of multifunctional monomers.²³ Although individual supramolecular bonds are relatively weak as compared to covalent bonds, multiple noncovalent interactions can work in concert to produce mechanically robust materials.²⁴ The importance of strong hydrogen bonding between macromolecules in nature is irrefutable: the structure and function of DNA and proteins are the result of hydrogen bonding and stacking interactions of nucleotides and amino acids, respectively. Specifically, the consequences of hydrogen bonding interactions can be observed in naturally derived materials; for example, the tensile strength of spider silk, which is produced by weak but numerous hydrogen bonds between proteins, is comparable to steel.25,26

The utility and susceptibility of hydrogen bonding has also been exploited in polymer networks to achieve robust synthetic materials; several studies demonstrate that the incorporation of hydrogen bonding moieties in synthetic polymers increases fatigue and heat resistance properties significantly. ^{27–30} In addition, the reversibility of these interactions leads to materials with stimuli-responsive behavior, adaptability, and the potential for self-healing and shape-memory capabilities. ^{31,32} Originally developed by Meijer and co-workers, 2-ureido-4[1H]-pyrimidinone (UPy), is a particularly promising hydrogen bonding moiety for the formation of supramolecular networks (Figure 1). High-affinity UPy dimers assemble in a self-complementary array of quadruple hydrogen bonds (Figure 1). ^{33–35} As such, Upy-terminated telechelic poly-

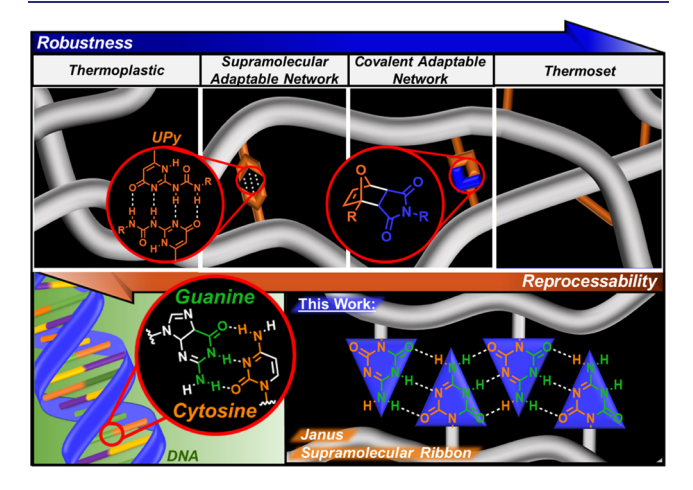


Figure 1. (Top) Depiction of thermoplastics, thermosets, and their intermediate counterparts based on either noncovalent (supramolecular networks) or dynamic-covalent (covalent adaptable networks) interactions. (Bottom) Prior work on hydrogen bonding supramolecular networks has focused on 1:1 pairing of 2-ureido-4[1*H*]-pyrimidinone (UPy) moieties, while the approach reported here relies on self-complementary hydrogen bonding of Janus guanine-cytosine base (GCB) groups.

mers,^{36–39} copolymers of acrylate and UPy-functionalized acrylate monomers,^{40–43} and polymers formed via postpolymerization functionalization with Upy moieties have been investigated for their utility in supramolecular networks.⁴⁴ However, the immiscibility of UPy monomers with appropriate solvents and other acrylate comonomers makes direct polymerization a challenging route to incorporate the Upymotif.⁴⁵ In addition to solvation challenges, similar to many dissociative CANs, supramolecular networks containing UPy motifs have been shown to lose connectivity at elevated temperatures (>160 °C), further limiting their applicability.^{29,30,46,47}

We reasoned that careful design of hydrogen bonded supramolecular networks can be utilized to preserve network structure even at elevated temperatures. Specifically, we envisioned that pendent groups capable of hydrogen bonding with more than one partner would collectively increase the temperature range of useful network performance. Recently, Sanjayan et al. developed a novel triazine-based Janus-faced guanine-cytosine base (GCB), comprised of two opposite faces, each representing the respective functionality of the quintessential guanine-cytosine DNA base pair. These GCB units were shown to form extended self-assemblies through 3 + 3 hydrogen bonding.⁴⁸ Like UPy, GCB exhibits a selfcomplementary hydrogen bonding sequence but with the added benefit that self-assembly of these moieties extends beyond 1:1 pairing, allowing the formation of extended ribbonlike structures (Figure 1). We hypothesized that incorporating the Janus GCB pendent groups into polymers would yield materials with an inherent equivalence of complementary selfassembling components and that this balance could be particularly advantageous when applied to copolymers in which the assembling units are highly diluted. Finally, with retention of the network structure, the GCB networks should flow via bond exchange, resulting in predictable viscoelastic flow (i.e., Arrhenius dependence) that is more commonly associated with associative networks (e.g., vitrimers)⁴⁹ and some dissociative networks.5

■ RESULTS AND DISCUSSION

To begin our investigation, we applied reversible additionfragmentation chain transfer (RAFT) polymerization of a tertbutyloxy carbonyl (boc)-protected guanine-cytosine basefunctionalized acrylate (GCBA_{boc}) and butyl acrylate (BA) to generate statistical copolymers P(BA-stat-GCBA_{boc}) of controlled molecular weight (Figure 2A). 51 To avoid contributions from physical cross-linking, we targeted polymers under the entanglement molecular weight of poly(butyl acrylate)⁵² and 5, 10, and 15 mol % GCBA_{boc} incorporation to yield copolymers denoted as $P(BA-stat-GCBA_{boc})_{x\%}$ (where x is the mol % incorporation of GCBA). During each copolymerization, the number-average molecular weight (M_n) of the prepolymers maintained uniform growth throughout the conversion, and low dispersity polymers were obtained. The pseudo-first-order kinetic plot was linear, and a monomodal shift in gel permeation chromatography (GPC) traces toward high molecular weight polymers was observed. These observations are good indicators of a controlled polymerization (Figure S1). Importantly, the consumption of GCBAboc and BA indicated similar monomer reactivities and, as such, the hydrogen bonding sites are expected to be evenly distributed along the polymer chains (Figure S1B). Finally, all three statistical copolymers with targeted number-average degree of polymer-

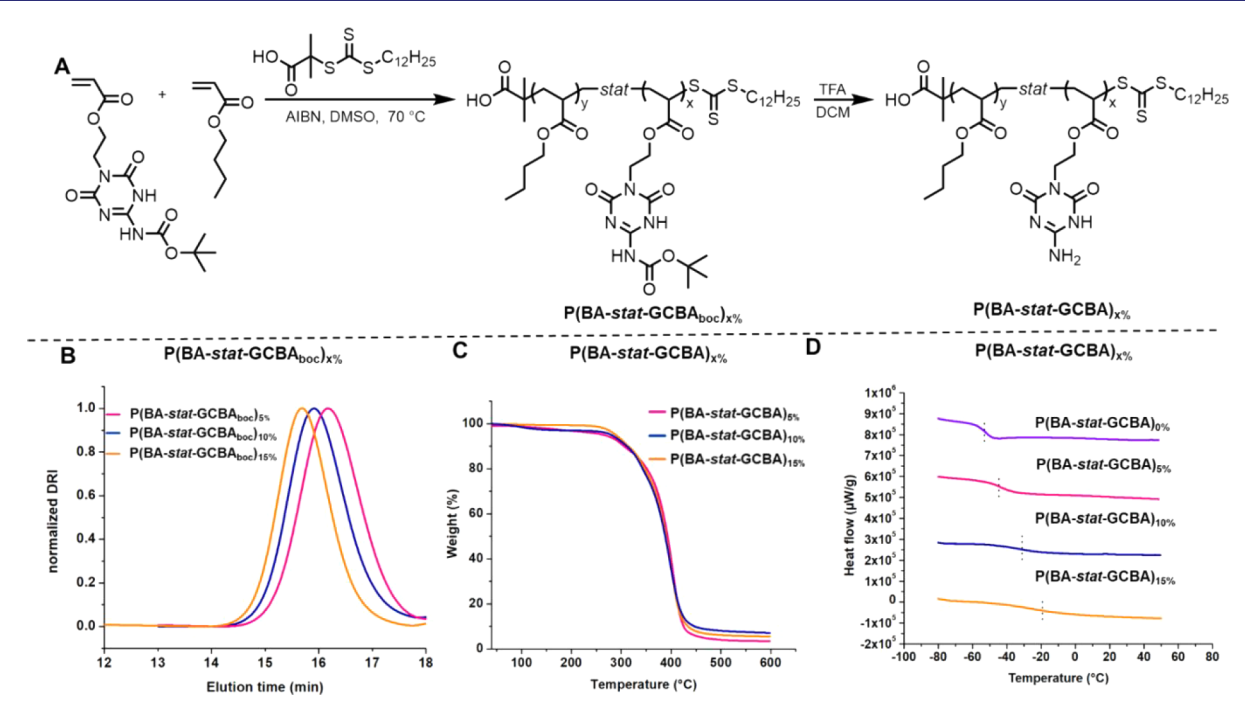


Figure 2. (A) General scheme for RAFT copolymerization of BA and GCBA_{boc} and subsequent deprotection; (B) GPC traces of P(BA-stat-GCBA_{boc})_{x%} statistical copolymers; (C) Thermogravimetric analysis plots and; (D) DSC thermograms of the polymers of boc-deprotected P(BA-stat-GCBA)_{x%} statistical copolymers.

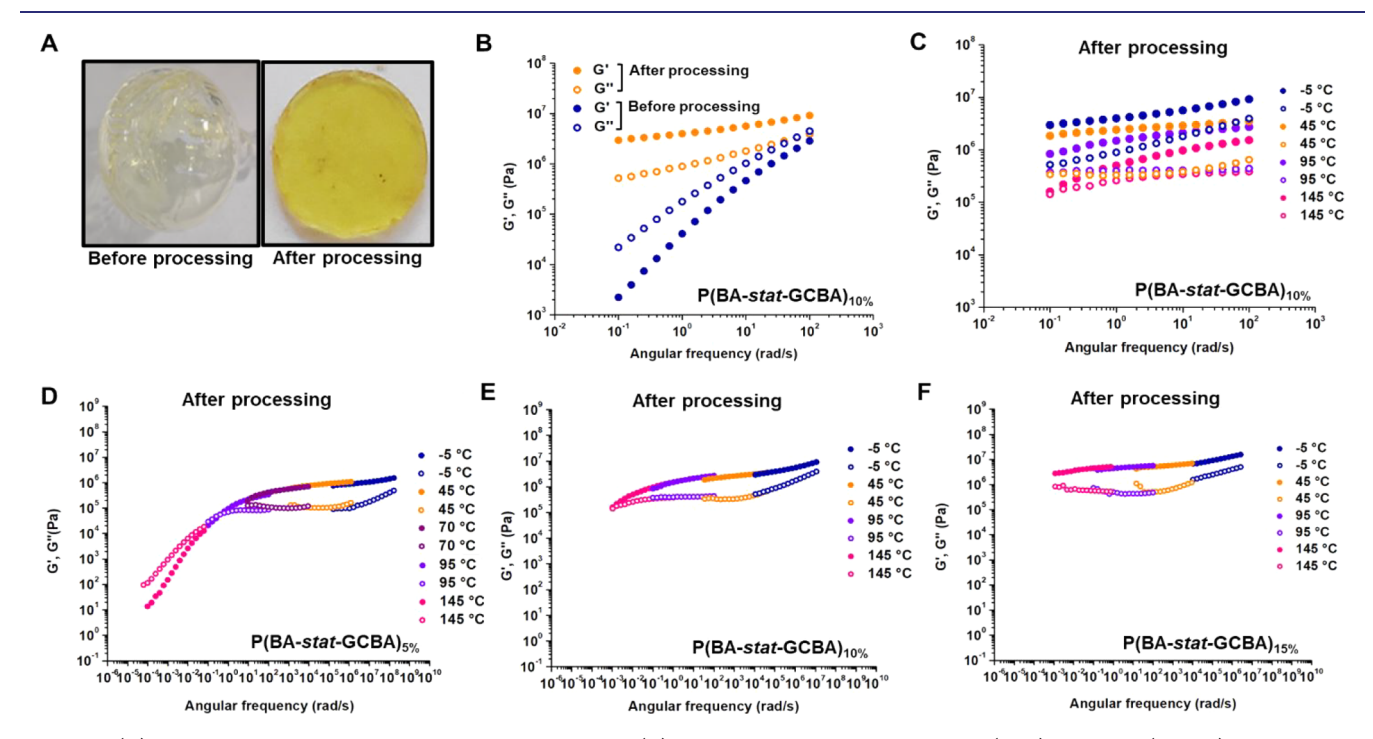


Figure 3. (A) Images of the samples before and after processing; (B) Storage and loss modulus before (blue) and after (orange) processing for $P(BA-stat-GCBA)_{10\%}$ at -5 °C; (C) Storage and loss modulus of $P(BA-stat-GCBA)_{10\%}$ from -5 to 145 °C; Time—temperature superposition master curves for (D) $P(BA-stat-GCBA)_{5\%}$; (E) $P(BA-stat-GCBA)_{10\%}$; and (F) $P(BA-stat-GCBA)_{15\%}$.

ization (DP) of 50 at 5, 10, and 15 mol % incorporation of $GCBA_{boc}$ were characterized by GPC (Figure 2B) and ^{1}H NMR spectroscopy (Table S2 and Figure S2).

With polymers in hand, the incorporated GCBA_{boc} units were deprotected using trifluoroacetic acid at room temperature to reveal polymers bearing the Janus-faced hydrogen bonding moiety (Figures S3–S4).^{S3} The thermal properties of the resulting materials were characterized by thermogravi-

metric analysis (TGA) and differential scanning calorimetry (DSC). TGA demonstrated excellent thermal stability, as indicated by only 5% degradation of the polymers at 270 °C (Figure 2C). DSC characterization revealed that the glass transition temperature ($T_{\rm g}$) of the copolymers increases with higher incorporation of GCBA. GCBA incorporations of 5, 10, and 15% exhibit a $T_{\rm g}$ of -45, -31, and -20 °C, respectively (Figure 2D). We attribute the increasing $T_{\rm g}$ with GCBA

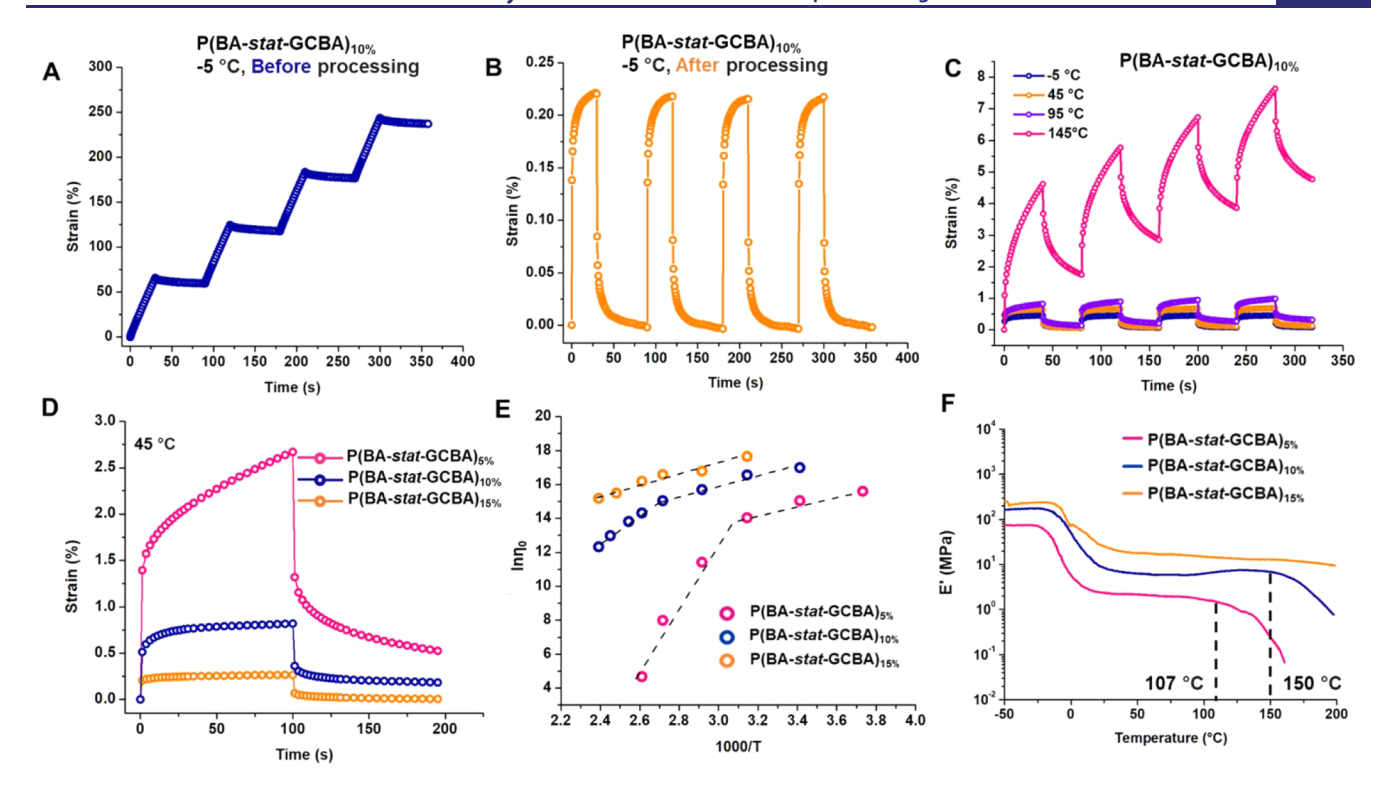


Figure 4. (A) Creep recovery experiments before processing of P(BA-stat-GCBA)_{10%} at -5 °C; (B) Creep recovery experiments after processing for P(BA-stat-GCBA)_{10%} at -5 °C; (C) Creep recovery experiments for P(BA-stat-GCBA)_{10%} at various temperatures; (D) Extended creep recovery experiments for P(BA-stat-GCBA)_{x%} samples at 45 °C; (E) Plot of ln η_0 vs 1000/T for P(BA-stat-GCBA)_{x%} samples; (F) Dynamic mechanical analysis (DMA) for P(BA-stat-GCBA)_{x%} samples.

incorporation to increasing degrees of higher intermolecular hydrogen bonding in the materials which restricts long-range segmental motion. 54

P(BA-stat-GCBA) at varying GCBA incorporations was solvent cast from dichloromethane to facilitate network formation and provide a baseline for thermomechanical analysis. The resulting films were compression molded at elevated temperatures (70, 90, and 120 °C for P(BA-stat-GCBA) at 5, 10, and 15% GCBA incorporation, respectively) (Figure 3A, S5) to remove residual solvent and to shape the material into disks and bars for further characterization. Initially, a control frequency sweep characterization on PBA at -5 °C demonstrated that material is a viscoelastic liquid at all frequencies (Figure S6). We expected that, with incorporation of GCBA in the PBA matrix, we would observe an increase of the elastic component in the system. Subsequently, we explored the effect of shear on the pre- and postprocessed materials at different temperatures by varying the frequency of an applied oscillatory strain (Figure 3). Frequency sweeps on $P(BA-stat-GCBA)_{10\%}$ at -5 °C revealed an increase in both the storage modulus (G') and loss modulus (G'') upon processing (Figure 3B). Additionally, the higher value of G' compared to G" after processing further indicated a transition from viscoelastic fluid to viscoelastic solid. This transition can be credited to the processing-induced self-assembly of hydrogen bonding motifs that formed cross-linked network structures. 55,56 Furthermore, we found that compression molding has a significant effect on the network formation of P(BA-stat- $GCBA)_{10\%}$. After solvent casting, the difference between G'and G'' was moderate, and with time we observed an increase in G' at -5 °C—which suggests with time a network is forming gradually in the system. Finally, after compression

molding, we obtained the maximum G' with an appreciable difference between G' and G'', indicating the formation of a percolated network (Figure S7). We continued these experiments by expanding the temperature range for each %GCBA incorporation (Figure 3C, S8A-B) and horizontally translating the modulus vs angular frequency spectra via time—temperature superposition with a reference temperature of 95 °C (Figure 3D-E). P(BA-stat-GCBA)_{5%} and P(BA-stat-GCBA)_{10%} displayed transitions from viscoelastic solids to viscoelastic fluids at 95 and 145 °C, respectively. This transition was not observed for P(BA-stat-GCBA)_{15%}, indicating the material remained a viscoelastic solid up to at least 145 °C within the tested frequencies (Figure 3F).

We further investigated P(BA-stat-GCBA) before and after processing by creep recovery experiments, where the material deformation (strain) from an applied constant force (stress) was observed over time. After the stress was released, the strain recovery was monitored to evaluate the extent of permanent deformation (i.e., creep). Prior to compression molding, P(BAstat-GCBA)_{10%} showed 65% deformation over just 30 s at -5 °C at a constant stress of 5000 Pa. Upon the release of the force the material recovered only 9% of the deformation, indicative of significant creep (Figure 4A). Following processing, P(BA-stat-GCBA)_{10%} showed only 0.2% deformation over the same duration and recovered over 98% of the deformation (Figure 4B). This finding is indicative of elastic recovery and consistent with results from the frequency sweep experiments. P(BA-stat-GCBA)_{10%}, both before and after processing, demonstrated consistent elastic behavior for three additional creep recovery cycles. Creep-recovery experiments were also utilized to understand the effect of compression molding. The result demonstrated that the solvent casted

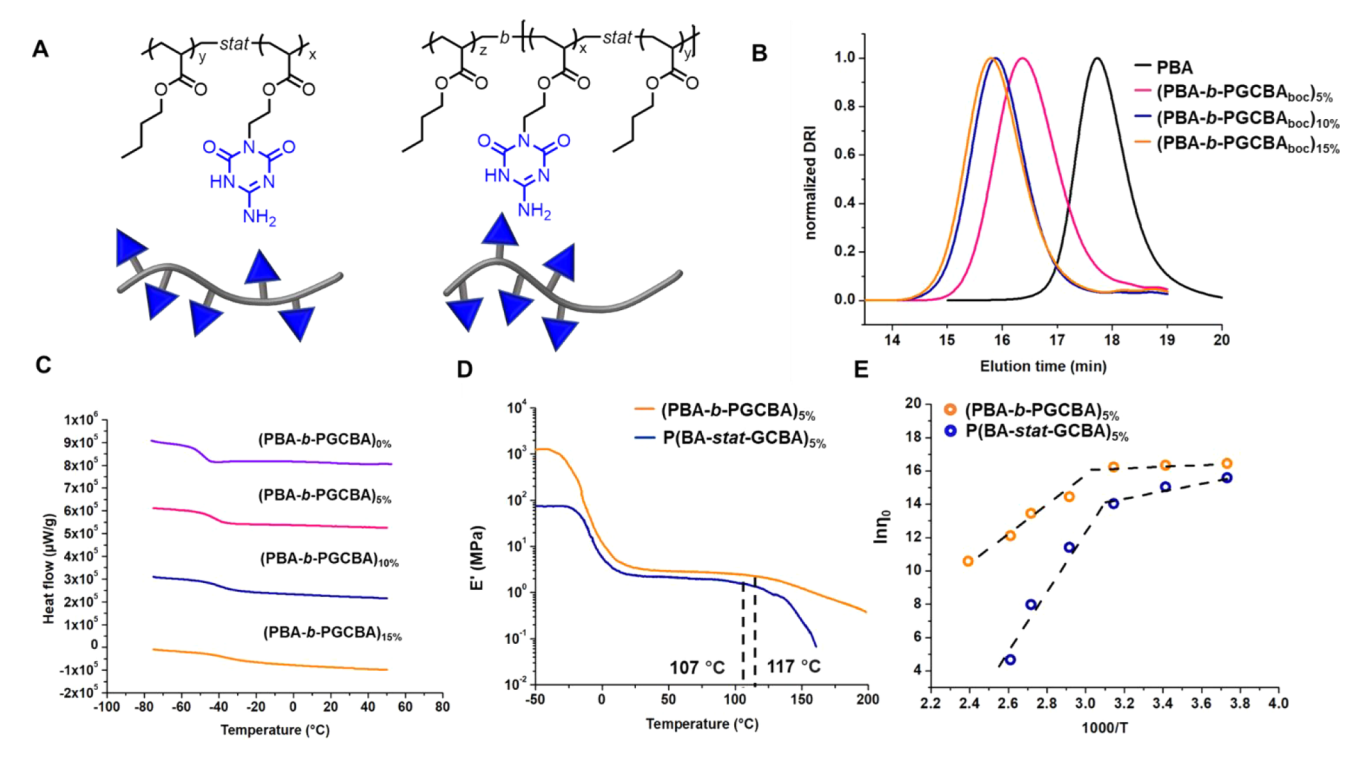


Figure 5. (A) Depiction of GCBA distribution in statistical and block copolymers; (B) GPC traces of PBA and (PBA-b-PGCBA_{boc})_{x%} samples; (C) DSC thermograms of (PBA-b-PGCBA)_{x%} samples; Comparison of the (D) DMA thermograms of block and statistical morphology at 5% incorporation of GCBA; (E) $\ln \eta_0$ vs 1000/T plot of block and statistical morphology at 5% incorporation of GCBA.

sample recovered only 83%, whereas the compression molded sample attained complete recovery at a constant stress of 10 kPa—indicating formation of a widespread network due to compression molding of the sample (Figure S9). P(BA-stat-GCBA)_{10%} was then subjected to creep recovery experiments at –5, 45, 95, and 145 °C at a constant stress of 10 000 Pa. An increase in permanent deformation—or viscous flow—was observed with increasing temperature. The effect was most pronounced above the temperature at which, according to the rheometric data, the polymer transitions from viscoelastic solid to viscoelastic fluid (Figure 4C, Figure S10–S11).⁵⁸

We then subjected processed P(BA-stat-GCBA) at 5, 10, and 15% GCBA incorporation to the same stress (10 000 Pa) for 100 s over a range of temperatures to evaluate flow behavior with respect to hydrogen bonding capability (Figure 4D, Figures S12-14). As expected, the flow rate of these materials decreased with increasing incorporation of GCBA, where cooperative interactions between hydrogen bonding moieties inhibit flow of the material. From this data, we extracted the zero-shear viscosity (η_0) at different temperatures from a compliance J(t) [creep/stress] vs time (t) plot following the equation, $J(t) = A + t/\eta_o$. For P(BA-stat-GCBA)_{5%}, a steady decrease of η_0 with increasing temperature up to 60 °C was observed, followed by a rapid decrease in η_o . The rapid reduction of η_o indicates the loss of network integrity due to disassociation of the GCBA moieties. The same trend was observed for P(BA-stat-GCBA)_{10%}, though the dramatic decline of η_o began at about 110 °C, suggesting the network structure is retained over a larger temperature range. For P(BA-stat-GCBA)_{15%}, no change in the flow behavior was observed suggesting retention of the network integrity over the entire temperature range (Figure 4E). We hypothesized that the difference in the slopes during network dissociation of P(BA-stat-GCBA)_{5%} and P(BA-stat-GCBA)_{10%} in Figure 4E

can be explained by cluster theory introduced by Semenov and Rubinstein. S9-61 With decreasing incorporation of GCBA cross-linkers, the polymer chains form loosely cross-linked clusters resulting in the sharpest decrease of viscosity after dissociation of the GCBA assembly. The activation energy for viscous flow $(E_{\rm a})$ was calculated from the initial flow dependence—prior to network disintegration—to be 24 \pm 2 kJ/mol for all the networks (Figure S15).

To conclude our look at how these processed statistical copolymer network structures perform at higher temperatures, we conducted temperature ramp experiments via DMA at oscillating strain (Figure 4F). The elastic rubbery plateau modulus (E_n) , extrapolated at the onset of the rubbery plateau in the thermogram, is related to the molecular weight between cross-links (M_x) of the network⁴⁰ (Figure S16), and the appearance of a dramatic decline in $E_{\rm n}$ at higher temperatures is indicative of network dissociation.³² The onset temperature of network dissociation $(T_{d-x\%}; x = \text{mol } \% \text{ incorporation of }$ GCBA in the polymer)⁴⁷ increases with increasing incorporation of GCBA ($T_{d-5\%}$ = 107 °C; $T_{d-10\%}$ = 150 °C) to such an extent that we did not observe network disintegration for P(BA-stat-GCBA) with 15% GCBA incorporation in the operating temperature range (-50-200 °C). To the best of our knowledge, this is the widest range of rubbery plateau ever reported for a supramolecular network showing excellent network integrity at elevated temperatures.⁴⁵ The elongated rubbery plateau observed for these systems was attributed to the cooperative effect of triplet hydrogen bond connectivity at each side of the GCBA cross-linker in concert with multiple self-assembled GCB units.⁶⁴ We hypothesize that face-to-face hydrogen bonding induces self-assembly of additional GCBA cross-linkers, generating a network that contains a higher effective number of cross-links per chain (N_c) than the number of GCBA units incorporated. To investigate this possibility, we

used the E_n and M_x data from DMA and M_n values from GPC to calculate the cross-link density (N_c) within these networks. As expected, an increase in cross-link density was observed with increasing GCBA content (Figure 4F). Interestingly, as the targeted mol % of GCBA increases to 15%, the N_c is strikingly higher than the number of average cross-linkers per chain (Table S4).65 The average number of GCBA units per chain is 3.6, 6.2, and 9.5 respectively at 5, 10, and 15% incorporation of GCBA. We see that for P(BA-stat-GCBA) at 5 and 10% GCBA, N_c is equal to or less than the number of GCBA units per chain i.e., 2 and 7, respectively. However, at 15% incorporation, N_c is 21, 2-fold greater than the number of GCBA units incorporated. We also used the G_n (the elastic rubbery plateau modulus from the frequency sweep master plots) which corroborates the N_c value calculated from DMA (Table S5). These results are strongly consistent with the ability of the GCBA units to interact with more than one partner with increasing incorporation and confers remarkable integrity to these networks.

To validate the hypothesis that hydrogen bonded Janusfaced GCBA units self-assemble beyond pairs, we investigated the effect of local GCBA concentration on network formation. We compared the thermomechanical properties of block copolymers of similar GCBA incorporation (5, 10, and 15 mol %, where the GCBA units were incorporated into only the second block) to their statistical counterparts (Figure 5A). We⁴⁹ and others⁶⁶ have previously shown that block copolymers in associative CANs exhibit higher creep-resistance compared to their statistical equivalent. We reasoned that a similar effect would be observed in this study given that an increase in local concentration of Janus cross-linkers would further increase the likelihood of extended hydrogen bonding over multiple GCBA units. The block copolymers were synthesized via RAFT polymerization (Figure 5B, Scheme S2, Table S6, Figure S18) using a macro-chain transfer agent (macro-CTA) PBA with a degree of polymerization of 25. This PBA macro-CTA was chain extended with BA and $GCBA_{boc}$ to target three different block copolymers with 5, 10, and 15 mol % incorporation of GCBA (PBA-b-PGCBA_{boc})_{x%} (where x is the mol % incorporation of GCBA). As with the statistical copolymers the total degree of polymerization was maintained at about 50 monomer units (Figure S18). Following amine deprotection, we observed that these block copolymers exhibited comparable $T_{\rm g}$ values to those of the statistical copolymers at similar compositions (Figure 5C). Obtaining rheometric data was limited to (PBA-b-PGCBA)_{5%} and (PBAb-PGCBA)_{10%}, as (PBA-b-PGCBA)_{15%} was incompressible at 130 °C, even after 16 h. Frequency sweeps revealed a greater increase in the magnitude for both G' and G'' after processing for (PBA-b-PGCBA)_{5%} and (PBA-b-PGCBA)_{10%} compared to their statistical counterparts.44 Furthermore, the rubbery plateau broadened upon changing the morphology from statistical to block copolymer indicating the formation of a more robust network (Figures S19-S20). Creep recovery experiments revealed that degrees of both creep and permanent deformation decreased in the block copolymer materials relative to the statistical copolymers (Figures S21-S24). DMA data also indicated both a greater cross-link density for block copolymer networks and a more gradual decline in the rubbery plateau at network disintegration (Figure 5D). The DMA exhibited the widest rubbery plateau for $(PBA-b-PGCBA)_{10\%}$, with network disintegration not being observed over the entire operating temperature range (Figure

S25A) (up to 200 °C). However, the statistical counterpart demonstrated network dissociation at the same incorporation of GCBA at around 150 °C. Accordingly, we reasoned that the GCBA local concentration is higher in the block copolymers, resulting in superior network integrity through the cooperative nature of higher order hydrogen bonding across multiple GCBA units. The higher local concentration of cross-links in the GCBA block preserves the network structure more effectively, as evidenced by a more gradual network disassociation transition in the DMA thermogram. This assertion was corroborated by the negligible reduction of η_o in the plot of $\ln(\eta_o)$ vs 1000/T at the lower temperature region and a less dramatic decrease of η_o at elevated temperatures (Figure 5E and Figure S25B).

To understand the versatility of this Janus cross-linker, we incorporated GCBA in a poly(methyl acrylate) (PMA) matrix where the degree of polymerization was kept constant at 50. The resulting P(MA-stat-GCBA_{boc})_{5%} polymer was characterized by GPC and ¹H NMR spectroscopy. After deprotection and processing of the sample, we characterized the network by DMA. The temperature ramp in DMA exhibited a rubbery plateau modulus with excellent network integrity up to 135 °C (Figure S26). The increased network degradation temperature with the PMA matrix demonstrates the potential of this system to be used with various monomers to obtain robust and reprocessable networks.

Lastly, we studied the recyclability of the networks through direct mechanical reprocessing. P(BA-stat-GCBA)_{5%} was broken into small fragments and compression molded for thermomechanical characterization (Figures S27–28). Negligible change of the storage modulus in the rubbery plateau region of DMA thermograms over three destruction/compression cycles suggests the absence of side reactions during recycling. Furthermore, recycled P(BA-stat-GCBA)_{5%} completely dissolved in dichloromethane over 24 h, highlighting the reversibility of network formation during material reprocessing conditions (Figures S29–30). With the retention of network structure over large temperature ranges while retaining solubility under mild conditions, these networks offer a unique alternative to more complex CAN counterparts.

SUMMARY AND CONCLUSIONS

Novel Janus-faced self-complementary hydrogen bonding motifs were explored in the synthesis of supramolecular networks of P(BA) using a self-assembling guanine-cytosine base-functionalized acrylate cross-linker. Rheological studies and DMA showed that the cooperative nature of hydrogen bonding in these networks yielded a spectrum of materials from viscoelastic liquid to solid and a tunable elastic rubbery plateau depending on the incorporation of GCBA cross-linkers. The network with the highest incorporation of GCBA, though only 15 mol %, displayed the widest rubbery plateau yet reported, to our knowledge, for a supramolecular network. To validate our claim that each Janus-faced moiety participates in multiple cross-links, we investigated the effect of local concentration of GCBA units on network integrity by comparing statistical and block copolymer morphology. The comparison study showed enhanced cross-linking of GCBA in block morphology due to the greater extent of GCBA selfassembly. This is the first report of the synthesis of extremely robust and tunable supramolecular networks through the synergistic effect of cross-linkers containing multiple binding sites per unit and self-assembly beyond dimers. We contend

that the cooperative nature of Janus-faced noncovalent bonding can be a powerful technique for the development of thermally robust supramolecular networks.

ASSOCIATED CONTENT

Supporting Information

The Supporting Information is available free of charge at https://pubs.acs.org/doi/10.1021/jacs.1c10606.

Materials, instrumentation, polymer synthesis, polymer characterization, network formation, rheology, dynamic mechanical analysis, and chemical recycling (PDF)

AUTHOR INFORMATION

Corresponding Authors

Brent S. Sumerlin — George & Josephine Butler Polymer Research Laboratory, Center of Macromolecular Science & Engineering, Department of Chemistry, University of Florida, Gainesville, Florida 32611, United States; ocid.org/ 0000-0001-5749-5444; Email: sumerlin@chem.ufl.edu

Gangadhar J. Sanjayan — Organic Chemistry Division, Council of Scientific and Industrial Research, National Chemical Laboratory (CSIR-NCL), Pune 411008, India; orcid.org/0000-0001-7764-7329; Email: gj.sanjayan@ncl.res.in

Authors

Swagata Mondal – George & Josephine Butler Polymer Research Laboratory, Center of Macromolecular Science & Engineering, Department of Chemistry, University of Florida, Gainesville, Florida 32611, United States

Jacob J. Lessard — George & Josephine Butler Polymer Research Laboratory, Center of Macromolecular Science & Engineering, Department of Chemistry, University of Florida, Gainesville, Florida 32611, United States; orcid.org/ 0000-0003-2962-6472

Chhuttan L. Meena – Organic Chemistry Division, Council of Scientific and Industrial Research, National Chemical Laboratory (CSIR-NCL), Pune 411008, India

Complete contact information is available at: https://pubs.acs.org/10.1021/jacs.1c10606

Author Contributions

§S.M. and J.J.L. contributed equally.

Notes

The authors declare no competing financial interest.

ACKNOWLEDGMENTS

This material is based upon work supported by the National Science Foundation (NSF DMR-1904631). Grant to G.J.S. (CSIR SSB-000726) is also gratefully acknowledged.

REFERENCES

- (1) Kloxin, C. J.; Bowman, C. N. Covalent adaptable networks: smart, reconfigurable and responsive network systems. *Chem. Soc. Rev.* **2013**, *42*, 7161–7173.
- (2) Podgorski, M.; Fairbanks, B. D.; Kirkpatrick, B. E.; McBride, M.; Martinez, A.; Dobson, A.; Bongiardina, N. J.; Bowman, C. N. Toward Stimuli-Responsive Dynamic Thermosets through Continuous Development and Improvements in Covalent Adaptable Networks (CANs). *Adv. Mater.* **2020**, *32*, 1906876.
- (3) Appel, E. A.; del Barrio, J.; Loh, X. J.; Scherman, O. A. Supramolecular polymeric hydrogels. *Chem. Soc. Rev.* **2012**, *41*, 6195–6214.

- (4) Herbst, F.; Dohler, D.; Michael, P.; Binder, W. H. Self-healing polymers via supramolecular forces. *Macromol. Rapid Commun.* **2013**, 34, 203–220.
- (5) Brutman, J. P.; Delgado, P. A.; Hillmyer, M. A. Polylactide Vitrimers. ACS Macro Lett. 2014, 3, 607–610.
- (6) Li, L.; Chen, X.; Jin, K.; Torkelson, J. M. Vitrimers Designed Both To Strongly Suppress Creep and To Recover Original Cross-Link Density after Reprocessing: Quantitative Theory and Experiments. *Macromolecules* **2018**, *51*, 5537–5546.
- (7) Guerre, M.; Taplan, C.; Nicolay, R.; Winne, J. M.; Du Prez, F. E. Fluorinated Vitrimer Elastomers with a Dual Temperature Response. *J. Am. Chem. Soc.* **2018**, *140*, 13272–13284.
- (8) Lessard, J. J.; Scheutz, G. M.; Hughes, R. W.; Sumerlin, B. S. Polystyrene-Based Vitrimers: Inexpensive and Recyclable Thermosets. *ACS Appl. Polym. Mater.* **2020**, *2*, 3044–3048.
- (9) Chen, X.; Dam, M.; Ono, K.; Mal, A.; Shen, H.; Nutt, S. R.; Sheran, K.; Wudl, F. A Thermally Re-mendable Cross-Linked Polymeric Material. *Science* **2002**, 295, 1698–1702.
- (10) Bowman, C. N.; Kloxin, C. J. Covalent adaptable networks: reversible bond structures incorporated in polymer networks. *Angew. Chem., Int. Ed.* **2012**, *51*, 4272–4274.
- (11) Kloxin, C. J.; Scott, T. F.; Adzima, B. J.; Bowman, C. N. Covalent Adaptable Networks (CANs): A Unique Paradigm in Crosslinked Polymers. *Macromolecules* **2010**, *43*, 2643–2653.
- (12) Röttger, M.; Domenech, T.; van der Weegen, R.; Breuillac, A.; Nicolaÿ, R.; Leibler, L. High-performance vitrimers from commodity thermoplastics through dioxaborolane metathesis. *Science* **2017**, *356*, 62–65.
- (13) Scheutz, G. M.; Lessard, J. J.; Sims, M. B.; Sumerlin, B. S. Adaptable Crosslinks in Polymeric Materials: Resolving the Intersection of Thermoplastics and Thermosets. *J. Am. Chem. Soc.* **2019**, *141*, 16181–16196.
- (14) Roy, N.; Bruchmann, B.; Lehn, J. M. DYNAMERS: dynamic polymers as self-healing materials. *Chem. Soc. Rev.* **2015**, 44, 3786—3807.
- (15) Heinzmann, C.; Weder, C.; de Espinosa, L. M. Supramolecular polymer adhesives: advanced materials inspired by nature. *Chem. Soc. Rev.* **2016**, *45*, 342–358.
- (16) Voorhaar, L.; Hoogenboom, R. Supramolecular polymer networks: hydrogels and bulk materials. *Chem. Soc. Rev.* **2016**, *45*, 4013–4031.
- (17) Whittell, G. R.; Hager, M. D.; Schubert, U. S.; Manners, I. Functional soft materials from metallopolymers and metallosupramolecular polymers. *Nat. Mater.* **2011**, *10*, 176–188.
- (18) Zhang, L.; Rowan, S. J. Effect of Sterics and Degree of Cross-Linking on the Mechanical Properties of Dynamic Poly(alkylurea—urethane) Networks. *Macromolecules* **2017**, *50*, 5051–5060.
- (19) Elling, B. R.; Dichtel, W. R. Reprocessable Cross-Linked Polymer Networks: Are Associative Exchange Mechanisms Desirable? *ACS Cent. Sci.* **2020**, *6*, 1488–1496.
- (20) Jourdain, A.; Asbai, R.; Anaya, O.; Chehimi, M. M.; Drockenmuller, E.; Montarnal, D. Rheological Properties of Covalent Adaptable Networks with 1,2,3-Triazolium Cross-Links: The Missing Link between Vitrimers and Dissociative Networks. *Macromolecules* **2020**, 53, 1884–1900.
- (21) Yan, X.; Wang, F.; Zheng, B.; Huang, F. Stimuli-responsive supramolecular polymeric materials. *Chem. Soc. Rev.* **2012**, *41*, 6042–6065.
- (22) Wang, S.; Urban, M. W. Self-healing polymers. *Nat. Rev. Mater.* **2020**, *5*, 562–583.
- (23) Li, S. L.; Xiao, T.; Lin, C.; Wang, L. Advanced supramolecular polymers constructed by orthogonal self-assembly. *Chem. Soc. Rev.* **2012**, *41*, 5950–5968.
- (24) Wojtecki, R. J.; Meador, M. A.; Rowan, S. J. Using the dynamic bond to access macroscopically responsive structurally dynamic polymers. *Nat. Mater.* **2011**, *10*, 14–27.
- (25) Rieth, L. R.; Eaton, R. F.; Coates, G. W. Polymerization of Ureidopyrimidinone-Functionalized Olefins by Using Late-Transition

- Metal Ziegler-Natta Catalysts: Synthesis of Thermoplastic Elastomeric Polyolefins. *Angew. Chem.* **2001**, *113*, 2211–2214.
- (26) Guerra, C. F.; Bickelhaupt, F. M.; Snijders, J. G.; Baerends, E. J. Hydrogen Bonding in DNA Base Pairs: Reconciliation of Theory and Experiment. *J. Am. Chem. Soc.* **2000**, *122*, 4117–4128.
- (27) Pan, Y.; Hu, J.; Yang, Z.; Tan, L. From Fragile Plastic to Room-Temperature Self-Healing Elastomer: Tuning Quadruple Hydrogen Bonding Interaction through One-Pot Synthesis. *ACS Appl. Polym. Mater.* **2019**, *1*, 425–436.
- (28) Bobade, S.; Wang, Y.; Mays, J.; Baskaran, D. Synthesis and Characterization of Ureidopyrimidone Telechelics by CuAAC "Click" Reaction: Effect of Tg and Polarity. *Macromolecules* **2014**, 47, 5040–5050.
- (29) Guo, M.; Pitet, L. M.; Wyss, H. M.; Vos, M.; Dankers, P. Y.; Meijer, E. W. Tough stimuli-responsive supramolecular hydrogels with hydrogen-bonding network junctions. *J. Am. Chem. Soc.* **2014**, 136. 6969–6977.
- (30) Tellers, J.; Canossa, S.; Pinalli, R.; Soliman, M.; Vachon, J.; Dalcanale, E. Dynamic Cross-Linking of Polyethylene via Sextuple Hydrogen Bonding Array. *Macromolecules* **2018**, *51*, 7680–7691.
- (31) Zhao, B.; Mei, H.; Liu, N.; Zheng, S. Organic–Inorganic Polycyclooctadienes with Double-Decker Silsesquioxanes in the Main Chains: Synthesis, Self-Healing, and Shape Memory Properties Regulated with Quadruple Hydrogen Bonds. *Macromolecules* **2020**, 53, 7119–7131.
- (32) Ware, T.; Hearon, K.; Lonnecker, A.; Wooley, K. L.; Maitland, D. J.; Voit, W. Triple-Shape Memory Polymers Based on Self-Complementary Hydrogen Bonding. *Macromolecules* **2012**, *45*, 1062–1069.
- (33) Sontjens, S. H. M.; Sijbesma, R. P.; van Genderen, M. H. P.; Meijer, E. W. Stability and Lifetime of Quadruply Hydrogen Bonded 2-Ureido-4[1H]-pyrimidinone Dimers. *J. Am. Chem. Soc.* **2000**, *122*, 7487–7493
- (34) Ligthart, G. B. W. L.; Ohkawa, H.; Sijbesma, R. P.; Meijer, E. W. Complementary Quadruple Hydrogen Bonding in Supramolecular Copolymers. *J. Am. Chem. Soc.* **2005**, *127*, 810–811.
- (35) Sijbesma, R. P.; Meijer, E. W. Quadruple hydrogen bonded systems. *Chem. Commun.* **2003**, 5–16.
- (36) Cao, K.; Liu, G. Low-Molecular-Weight, High-Mechanical-Strength, and Solution-Processable Telechelic Poly(ether imide) End-Capped with Ureidopyrimidinone. *Macromolecules* **2017**, *50*, 2016–2023.
- (37) Yamauchi, K.; Kanomata, A.; Inoue, T.; Long, T. E. Thermoreversible Polyesters Consisting of Multiple Hydrogen Bonding (MHB). *Macromolecules* **2004**, *37*, 3519–3522.
- (38) Chang, R.; Shan, G.; Bao, Y.; Pan, P. Enhancement of Crystallizability and Control of Mechanical and Shape-Memory Properties for Amorphous Enantiopure Supramolecular Copolymers via Stereocomplexation. *Macromolecules* **2015**, *48*, 7872–7881.
- (39) Hutin, M.; Burakowska-Meise, E.; Appel, W. P. J.; Dankers, P. Y. W.; Meijer, E. W. From Molecular Structure to Macromolecular Organization: Keys to Design Supramolecular Biomaterials. *Macromolecules* **2013**, *46*, 8528–8537.
- (40) Lewis, C. L.; Stewart, K.; Anthamatten, M. The Influence of Hydrogen Bonding Side-Groups on Viscoelastic Behavior of Linear and Network Polymers. *Macromolecules* **2014**, *47*, 729–740.
- (41) Li, J.; Lewis, C. L.; Chen, D. L.; Anthamatten, M. Dynamic Mechanical Behavior of Photo-Cross-linked Shape-Memory Elastomers. *Macromolecules* **2011**, *44*, 5336–5343.
- (42) Cummings, S. C.; Dodo, O. J.; Hull, A. C.; Zhang, B.; Myers, C. P.; Sparks, J. L.; Konkolewicz, D. Quantity or Quality: Are Self-Healing Polymers and Elastomers Always Tougher with More Hydrogen Bonds? ACS Appl. Polym. Mater. 2020, 2, 1108–1113.
- (43) Jankova, K.; Javakhishvili, I.; Kobayashi, S.; Koguchi, R.; Murakami, D.; Sonoda, T.; Tanaka, M. Hydration States and Blood Compatibility of Hydrogen-Bonded Supramolecular Poly(2-methoxyethyl acrylate). ACS Appl. Bio Mater. 2019, 2, 4154–4161.

- (44) Feldman, K. E.; Kade, M. J.; Meijer, E. W.; Hawker, C. J.; Kramer, E. J. Model Transient Networks from Strongly Hydrogen-Bonded Polymers. *Macromolecules* **2009**, *42*, 9072–9081.
- (45) Heinzmann, C.; Lamparth, I.; Rist, K.; Moszner, N.; Fiore, G. L.; Weder, C. Supramolecular Polymer Networks Made by Solvent-Free Copolymerization of a Liquid 2-Ureido-4[1H]-pyrimidinone Methacrylamide. *Macromolecules* **2015**, *48*, 8128–8136.
- (46) Wei, M.; Zhan, M.; Yu, D.; Xie, H.; He, M.; Yang, K.; Wang, Y. Novel poly(tetramethylene ether)glycol and poly(epsilon-caprolactone) based dynamic network via quadruple hydrogen bonding with triple-shape effect and self-healing capacity. *ACS Appl. Mater. Interfaces* **2015**, *7*, 2585–2596.
- (47) Watts, A.; Hillmyer, M. A. Aliphatic Polyester Thermoplastic Elastomers Containing Hydrogen-Bonding Ureidopyrimidinone Endgroups. *Biomacromolecules* **2019**, 20, 2598–2609.
- (48) Meena, C. L.; Singh, D.; Kizhakeetil, B.; Prasad, M.; George, M.; Tothadi, S.; Sanjayan, G. J. Triazine-Based Janus G-C Nucleobase as a Building Block for Self-Assembly, Peptide Nucleic Acids, and Smart Polymers. *J. Org. Chem.* **2021**, *86*, 3186–3195.
- (49) Lessard, J. J.; Scheutz, G. M.; Sung, S. H.; Lantz, K. A.; Epps, T. H., 3rd; Sumerlin, B. S. Block Copolymer Vitrimers. *J. Am. Chem. Soc.* **2020**, *142*, 283–289.
- (50) Chakma, P.; Morley, C. N.; Sparks, J. L.; Konkolewicz, D. Exploring How Vitrimer-like Properties Can Be Achieved from Dissociative Exchange in Anilinium Salts. *Macromolecules* **2020**, *53*, 1233–1244.
- (51) Moad, G.; Rizzardo, E.; Thang, S. H. Living Radical Polymerization by the RAFT Process. *Aust. J. Chem.* **2005**, *58*, 379–410.
- (52) Zhuge, F.; Brassinne, J.; Fustin, C.-A.; van Ruymbeke, E.; Gohy, J.-F. Synthesis and Rheology of Bulk Metallo-Supramolecular Polymers from Telechelic Entangled Precursors. *Macromolecules* **2017**, *50*, 5165–5175.
- (53) Roy, S. G.; Acharya, R.; Chatterji, U.; De, P. RAFT polymerization of methacrylates containing a tryptophan moiety: controlled synthesis of biocompatible fluorescent cationic chiral polymers with smart pH-responsiveness. *Polym. Chem.* **2013**, *4*, 1141–1152.
- (54) Kuo, S.-W.; Tsai, H.-T. Complementary Multiple Hydrogen-Bonding Interactions Increase the Glass Transition Temperatures to PMMA Copolymer Mixtures. *Macromolecules* **2009**, 42, 4701–4711.
- (55) Joshi, N.; Suman, K.; Joshi, Y. M. Rheological Behavior of Aqueous Poly(vinyl alcohol) Solution during a Freeze-Thaw Gelation Process. *Macromolecules* **2020**, *53*, 3452-3463.
- (56) Golkaram, M.; Fodor, C.; van Ruymbeke, E.; Loos, K. Linear Viscoelasticity of Weakly Hydrogen-Bonded Polymers near and below the Sol-Gel Transition. *Macromolecules* **2018**, *51*, 4910–4916.
- (57) Shabbir, A.; Javakhishvili, I.; Cerveny, S.; Hvilsted, S.; Skov, A. L.; Hassager, O.; Alvarez, N. J. Linear Viscoelastic and Dielectric Relaxation Response of Unentangled UPy-Based Supramolecular Networks. *Macromolecules* **2016**, *49*, 3899–3910.
- (58) Chen, Y.; Kushner, A. M.; Williams, G. A.; Guan, Z. Multiphase design of autonomic self-healing thermoplastic elastomers. *Nat. Chem.* **2012**, *4*, 467–472.
- (59) Rubinstein, M.; Semenov, A. N. Thermoreversible Gelation in Solutions of Associating Polymers. 2. Linear Dynamics. *Macromolecules* **1998**, *31*, 1386–1397.
- (60) Kuang, X.; Liu, G.; Dong, X.; Wang, D. Correlation between stress relaxation dynamics and thermochemistry for covalent adaptive networks polymers. *Mater. Chem. Front.* **2017**, *1*, 111–118.
- (61) Sheridan, R. J.; Bowman, C. N. A Simple Relationship Relating Linear Viscoelastic Properties and Chemical Structure in a Model Diels—Alder Polymer Network. *Macromolecules* **2012**, *45*, 7634—7641.
- (62) Fischer, P.; Rehage, H. Rheological Master Curves of Viscoelastic Surfactant Solutions by Varying the Solvent Viscosity and Temperature. *Langmuir* **1997**, *13*, 7012–7020.
- (63) Pletneva, V. A.; Molchanov, V. S.; Philippova, O. E. Effect of polymer on rheological behavior of heated solutions of potassium oleate cylindrical micelles. *Colloid J.* **2010**, 72, 716–722.

- (64) Stokely, K.; Mazza, M. G.; Stanley, H. E.; Franzese, G. Effect of hydrogen bond cooperativity on the behavior of water. *Proc. Natl. Acad. Sci. U.S.A.* **2010**, *107*, 1301–1306.
- (65) Gluck-Hirsch, J. B.; Kokini, J. L. Determination of the molecular weight between crosslinks of waxy maize starches using the theory of rubber elasticity. *J. Rheol.* **1997**, *41*, 129–140.
- (66) Ishibashi, J. S. A.; Pierce, I. C.; Chang, A. B.; Zografos, A.; El-Zaatari, B. M.; Fang, Y.; Weigand, S. J.; Bates, F. S.; Kalow, J. A. Mechanical and Structural Consequences of Associative Dynamic Cross-Linking in Acrylic Diblock Copolymers. *Macromolecules* **2021**, 54, 3972–3986.